

See discussions, stats, and author profiles for this publication at: <https://www.researchgate.net/publication/231632337>

Photoluminescence of C₆₀ and Its Photofragments in the Gas Phase

ARTICLE *in* THE JOURNAL OF PHYSICAL CHEMISTRY A · MAY 2002

Impact Factor: 2.69 · DOI: 10.1021/jp0146871

CITATIONS

3

READS

19

3 AUTHORS, INCLUDING:



Young Jong Lee

National Institute of Standards and Technolo...

46 PUBLICATIONS 918 CITATIONS

SEE PROFILE



Nam Woong Song

72 PUBLICATIONS 657 CITATIONS

SEE PROFILE

Photoluminescence of C₆₀ and Its Photofragments in the Gas Phase

Young Jong Lee, Nam Woong Song,[†] and Seong Keun Kim*

School of Chemistry, Seoul National University, Seoul 151-747, Korea

Received: December 31, 2001; In Final Form: March 26, 2002

The genuine photoluminescence spectrum of the S₁ state of C₆₀ was observed for the first time in the gas phase, using laser-induced fluorescence by photoexcitation at 266, 355, and 532 nm. The authenticity of the photoluminescence spectrum was confirmed by the sublimation enthalpy of the emitting species, the linear fluence dependence of emission intensity, the single exponential temporal decay of emission, and the constancy of the spectrum over different time delays and different excitation wavelengths. Upon increasing the laser fluence, drastically different emission features emerged. With photoexcitation at 266 nm, two spectral series with narrow bandwidths and fast decay times were observed on top of a broad emission band, which were identified as the Swan band and the Fox-Herzberg band of C₂ photofragmented from C₆₀. The broad band was deconvoluted into three component bands that persisted beyond time scales longer than a microsecond. In contrast, by photoexcitation at 355 nm, only the broad underlying emission was observed. From the fluence dependence and temporal profiles of the sharp and broad emission bands, generation mechanisms of the emitting species were proposed.

I. Introduction

Despite the extensive studies on the optical and spectroscopic properties of C₆₀ in the condensed phase over the past decade, surprisingly little is known about these properties in the gas phase. This is mainly due to the low vapor pressure and thus low number density of the molecule in the gas phase under typical experimental conditions. The absorption spectra of C₆₀ in the gas phase have been measured in the ultraviolet (UV)^{1–3} and visible^{4,5} regions, but no fluorescence spectrum from its S₁ state has been reported to date in the gas phase. The electronic transition between the S₀ and S₁ states is known to be symmetry-forbidden.⁶

On the other hand, optical emission studies have been carried out in the gas phase on super-hot C₆₀ and its fragments generated by a large amount of energy in the form of multiphoton absorption,^{7–9} electron impact,¹⁰ rf plasma,¹¹ and laser desorption.¹² The emission spectrum and its characteristics were found to depend strongly on experimental conditions such as, for example, laser wavelength, fluence, and pulse duration in the case of multiphoton absorption. Such strong dependence is generally attributed to the complexity of the various competing processes that lead to the cooling of the super-hot C₆₀, which may include fragmentation, ionization, and emission of radiation. For instance, fragmentation (or “evaporation”) of C₂ from C₆₀ is one of the principal cooling processes of interest in mass spectrometry,^{13,14} and, in some cases, optical emission has been observed from the fragmented C₂ unit.^{7,9,12} Broad and long-lived emission from super-hot C₆₀ has also been observed and attributed to blackbody radiation on the basis of its spectral position and spectral shift upon cooling.^{8–10,12}

In this work, we report for the first time the hitherto unknown fluorescence spectrum of C₆₀ in the gas phase. We also discuss

the emission from major photofragmentation products of C₆₀, including C₂ and possibly larger species, and their generation mechanisms.

II. Experimental Section

The experimental apparatus used in this work consisted of a vacuum chamber with an effusion source for C₆₀, a laser, and a detection system. The chamber was typically maintained at a pressure of 5×10^{-6} Torr. The C₆₀ powder was purchased from Hoechst Chemical Co. (gold grade, 99.6%), and the residual solvent was completely removed before use by baking the powder at 350 °C for 2 h. For the test measurement of photoluminescence from a solid film, a C₆₀ film of 0.5-μm thickness was deposited by thermal evaporation of the C₆₀ powder onto a quartz plate for 1 h at 450 °C. An effusive beam of C₆₀ was generated through a 2-mm hole of a sample reservoir whose temperature was varied over 450–700 °C, with a corresponding vapor pressure of 8.6×10^{-5} to 2.6×10^{-1} Torr, or an equivalent number density of 2.9×10^9 to 6.4×10^{12} cm⁻³. We used harmonics (532, 355, 266 nm) of a Q-switched Nd:YAG laser (6-ns pulse width, 10-Hz repetition rate, 7-mm beam diameter) for photoexcitation. Sapphire windows were fitted to the ends of the three arms of the chamber, transmitting the UV and visible light. To reduce the background due to the scattered laser light, the windows were positioned at the Brewster angle and several light baffles were placed inside the arms. Photoluminescence from C₆₀ was collected by using a lens perpendicular to the laser beam direction, introduced to a monochromator, and detected by a photomultiplier tube. The spectral resolution of the monochromator could be varied from 0.1 to 6 nm. The spectral range of the photomultiplier tube was from 200 to 850 nm. For the emission from the S₁ state, a 550-nm long-pass filter was used in front of the entrance slit of the monochromator to block the Rayleigh scattering as well as the photoluminescence from the sapphire windows over 300–500 nm. The signal from the photomultiplier tube was fed into a gated integrator/signal averager. When measuring the temporal

* Corresponding author. Fax: +82-2-889-5719. E-mail: seongkim@plaza.snu.ac.kr.

[†] Present address: Laser Metrology Group, Korea Research Institute of Standards and Science, Taejeon 305-600, Korea.

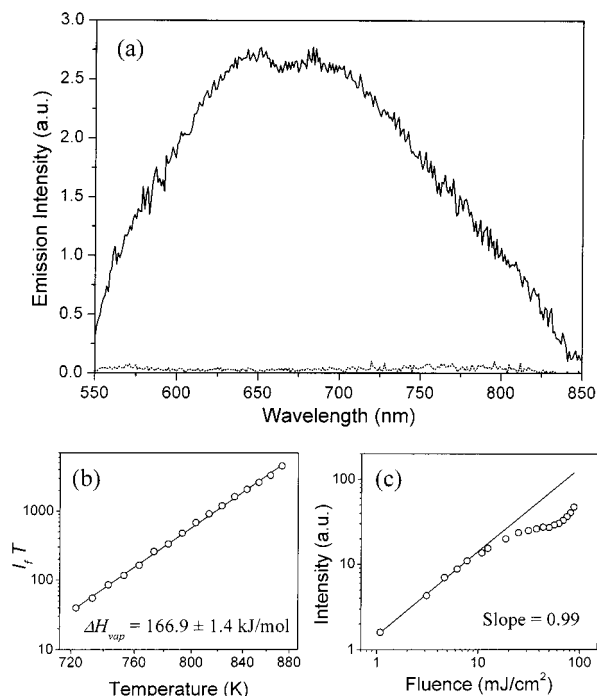


Figure 1. (a) Photoluminescence spectrum of C₆₀ in the gas-phase excited by the 355-nm light with a fluence of 6.2 mJ/cm² at the sample temperature of 600 °C (solid curve) and the background emission measured at room temperature (dotted curve). (b) Plot of $\log(I_f T)$ vs $1/T$, where I_f is the photoluminescence intensity, and T , temperature. The intensity of emission from the gas-phase C₆₀ excited by the 266-nm light with a fluence of 3 mJ/cm² was measured at 700 nm over the sample temperature range of 450–600 °C. (c) A log–log plot of the photoluminescence intensity at 700 nm vs laser fluence at 355 nm. The slope of the linear region is 0.99, indicating that the emission is due to a single photon process in this range of fluence.

profile of the photoluminescence, a 1-GHz digital storage oscilloscope was used.

III. Results and Discussion

1. Photoluminescence of C₆₀ in the Gas Phase. A photoluminescence spectrum of C₆₀ in the gas phase is shown in Figure 1a by a solid line. To confirm that it is a genuine fluorescence spectrum from the S₁ state of C₆₀ in the gas phase, the following set of tests were performed.

No Contamination by the Background Emission. The spectrum shown by the dotted line in Figure 1a was obtained under the conditions identical to those used for the solid line spectrum, except that the former was obtained with the sample at room temperature. The very low intensity of the dotted-line spectrum means that the solid-line spectrum contains virtually no background. Possible sources of the background emission may include scattered light and photoluminescence of C₆₀ in any phase other than gas. Because the density of C₆₀ deposited on the inner walls of the chamber was much higher than that of C₆₀ in our effusive beam, great care was taken to reduce the laser scattering inside the chamber and also to avoid photoluminescence from the C₆₀ deposited on chamber walls. For every gas-phase spectrum in this paper, it was positively confirmed that no background emission was included in our photoluminescence spectrum by measuring the emission with the sample at room temperature.

Sublimation Enthalpy of the Emitting Species. If the sample vapor behaves like an ideal gas and its fluorescence quantum yield does not depend on temperature, the following modified Clausius–Clapeyron equation can be applied to obtaining the

TABLE 1: The Sublimation Enthalpies of C₆₀

method ^a	ΔH_{sub} (kJ/mol)	T (K)	ref
TD	138.5 ± 3.8	550–600	52
KEMS	168 ± 5	640–800	53
AS	180 ± 10	819–995	4
KETG	159 ± 4	673–873	54
KEMS	181.4 ± 2.3	600–800	55
KEMS	158 ± 3	652–779	56
TE and KETG	175.3 ± 2.9	730–990	57
AS ^b	175	673–1013	2
AS ^b	150 ± 20	810–907	5
ES	166.9 ± 1.4	723–873	this work

^a TD: thermal desorption; KEMS: Knudsen-effusion mass spectrometry; TGA: thermogravimetric analysis; KETG: Knudsen-effusion thermogravimetry; AS: absorption spectroscopy; TE: torsion effusion; ES: emission spectroscopy. ^b These values are underestimated because the sublimation enthalpy was obtained from the relation between $\log A$ vs $1/T$ (A being the absorbance), not from its correct form, $\log(AT)$ vs $1/T$.

sublimation enthalpy ΔH_{vap} of the emitting species from the emission intensity I_f and temperature T :⁴

$$\log(I_f T) = A - \frac{\Delta H_{\text{vap}}}{R \ln 10} \times \frac{1}{T}$$

where R is the ideal gas constant, and A is another constant. The emission intensity at 700 nm was measured over the temperature range of 450–600 °C, and $\log(I_f T)$ was plotted against $1/T$ in Figure 1b. A good linearity is clearly seen in the plot, and its slope gives ΔH_{vap} of 166.9 ± 1.4 kJ/mol. This value of the sublimation enthalpy for C₆₀ is in good agreement with other values previously obtained by various methods (Table 1). The sublimation enthalpy did not vary much over different emission wavelengths. It means that there is only one major emitting species, which is most likely the gas-phase C₆₀, judging from the value of the sublimation enthalpy.

Laser Fluence Dependence. The fluence dependence of the emission intensity in the log–log plot of Figure 1c exhibits a linear behavior with a slope of 0.99 in the fluence range of 1–8 mJ/cm² at 355 nm. Such a linear dependence means that the emission comes from an excited state generated by a single photon process. On the other hand, in the fluence range of 10 to 60 mJ/cm², the emission intensity increases much more slowly and appears to reach a plateau, indicating saturation of the emission from the single photon process. At still higher fluences beyond 60 mJ/cm², however, the curve rises again, this time with a slope even higher than unity, which implies that other emitting channels become open upon multiphoton absorption. In a previous study, emission of a photon from the gas-phase C₆₀ excited by 193 nm showed a power dependence with an exponent larger than two in the fluence range of 3 to 80 mJ/cm², which was assigned as a blackbody-type light emission.⁸ It is clear that our emission spectrum in Figure 1a results from genuine one-photon absorption at a low fluence, while at high fluences, other emitting species are presumed to be generated by multiphoton absorption and contribute to the emission spectrum. Generation of these other emitting species at a high fluence will be discussed later.

Invariance of the Spectrum by Different Excitation Wavelengths. Figure 2a shows that the emission spectra obtained with different excitation wavelengths of 266, 355, and 532 nm have very similar spectral shapes. The spectra were all confirmed to be generated by a single photon absorption process. This is a typical Kasha's rule behavior,¹⁵ and explicitly rules out the possibility of blackbody radiation, whose spectrum shifts as the

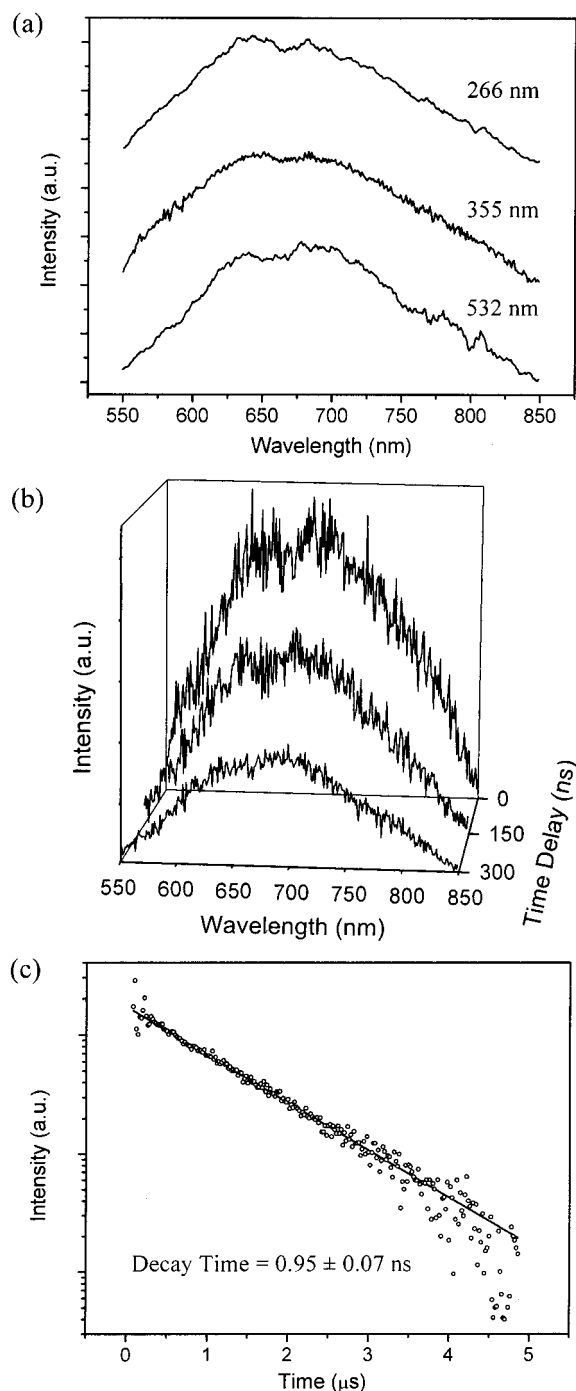


Figure 2. (a) Photoluminescence spectra of C₆₀ excited at three different wavelengths shown. All spectra have nearly identical spectral shape. It was also confirmed that they were all generated by the single photon absorption. (b) Time-dependent spectra of C₆₀ excited at 266 nm measured at time delays of 0, 150, and 300 ns, which shows the constancy of the spectrum over time. (c) Temporal profile of the photoluminescence excited at 266 nm and measured at 700 nm. The decay was nearly single exponential, with a decay time of 0.95 μs. The laser fluence used for (b) and (c) was a few mJ/cm² at 266 nm.

internal temperature varies,^{8,9} i.e., as the excitation energy is changed. Therefore, the character of the emission must be fluorescence or phosphorescence, which occurs from the lowest excited state with a singlet or triplet multiplicity.

Although phosphorescence of C₆₀ in the gas phase has not been reported yet, the energy of the lowest triplet state has been determined under various conditions. In a supersonic beam, the energy of the lowest triplet state of C₆₀ was reported to be 1.70

eV (13700 cm⁻¹, 730 nm) using photoelectron spectroscopy.¹⁶ The origin wavelength of phosphorescence was measured to be 782.92 nm (12773 cm⁻¹) in a Ne matrix,¹⁷ 798.1 nm (12530 cm⁻¹) in a Decaline/cyclohexane glass,¹⁸ and 862 nm (11600 cm⁻¹) in a single crystal.¹⁸ By comparison, our emission centered at around 660 nm with a blue-edge of 550 nm is too far off from these values, and thus phosphorescence is ruled out as a possible origin of the emission.

Like phosphorescence, fluorescence of C₆₀ has not been observed in the gas phase, but the energy of its S₁ state has been estimated in various ways. Catalán¹⁹ predicted the position of the absorption band origin of C₆₀ to be at 607.3 ± 0.2 nm in the gas phase by extrapolation of the absorption bands and the corresponding Lorenz-Lorenz functions for a series of *n*-alkane solvents. From the resonant two-photon ionization (R2PI) spectroscopy of C₆₀ in molecular beams, Hauffler et al. observed sharp peaks near 600 nm due to vibronically allowed transitions, although no origin was explicitly assigned.²⁰ Sassara et al. measured absorption and dispersed/excitation fluorescence spectra of C₆₀ in Ne and Ar matrixes, and from comparison of their spectra with the gas-phase R2PI spectrum,¹⁶ they estimated the 0–0 transition in the gas phase at 15696 ± 5 cm⁻¹ (637.10 nm).^{21,22} If we assign our emission as fluorescence, the significant discrepancy between the onset wavelength of 550 nm (18000 cm⁻¹) in our spectrum and the estimated singlet origin of 637.10 nm could be justified by the high vibrational temperature in the excited state due to the high initial temperature and excess photon energy. In fact, the extremely broad spectral range of the emission may also have the same origin.

Single-Exponential Decay of Emission in Time-Resolved Spectroscopy. We obtained a set of time-dependent spectra for C₆₀ with different time delays, but their spectral shape was nearly identical, as shown in Figure 2b. We also obtained a temporal profile of the emission, which is shown in Figure 2c that reveals a perfect single exponential decay. These results indicate that the emission contains only one transition from one electronically excited state.

The fitted decay time for the emission of C₆₀ at 700 nm was 0.95 ± 0.07 μs. This value is about 1000 times longer than the fluorescence lifetime of C₆₀ in toluene solution (1.17 ns²³ and 1.3 ns²⁴), and about 40 and 100 times shorter than the phosphorescence lifetime in a supersonic beam (42 μs¹⁶) and in a solid Ne matrix (90 μs¹⁷), respectively. Since the S₁–S₀ transition of C₆₀ is symmetry-forbidden,⁶ perturbation applied in solution should enhance both radiative and nonradiative transition rates, which decreases the fluorescence lifetime in solution.

2. Spectral Features of the Emission. Since we have presented pieces of evidence that the emission we observed was genuine fluorescence of C₆₀ in the gas phase, we now address the properties of this emission and its spectral features. In Figure 3, the fluorescence spectrum of C₆₀ in the gas phase, (Figure 3a), is compared with those of C₆₀ in the benzene solution and C₆₀ film on glass (Figure 3b,c), respectively]. All three spectra were obtained after being excited by the 355 nm light, and the spectra of the benzene solution and solid film were observed at room temperature. The spectral shifts of the peak maximum for the benzene solution and the solid film are 830 and 1700 cm⁻¹, respectively, with respect to the gas-phase fluorescence. Such a large red shift from the gas phase occurs often due to the increased dipole moment of the excited state, reorientation of the solvent molecules in the excited state, and specific interactions such as hydrogen bonding and complexation.²⁵ In the case of C₆₀, however, the dipole moments of both the ground

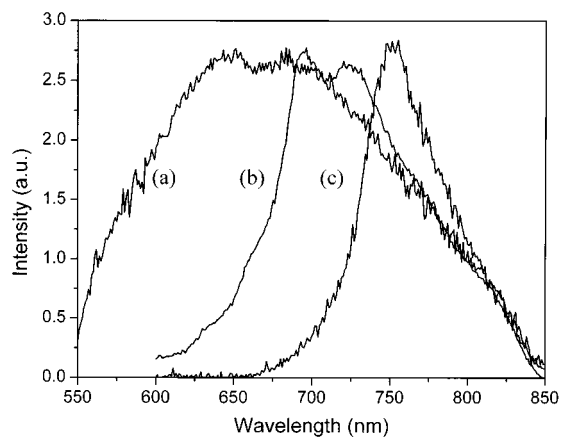


Figure 3. Comparison of photoluminescence spectra of C₆₀ in (a) the gas phase, (b) the benzene solution, and (c) the solid film on glass. All spectra were obtained by excitation at 355 nm. The spectrum (a) was measured at a sample temperature of 600 °C, while the other two spectra were taken at room temperature.

and excited states are known to be zero, and there is no specific interaction between the chromophore and the solvent. Only the dispersion forces are expected to contribute to the solvation of a nonpolar solute by nonpolar solvents. In this case, the solvent shift is generally known to be 70–3000 cm⁻¹ to the red with respect to the vapor phase.²⁶ Catalán¹⁹ found a good linear relation between the positions of the absorption band of C₆₀ in solution and the corresponding Lorenz–Lorentz functions, $f(n^2) = (n^2 - 1)/(n^2 + 2)$, for the *n*-alkane solvents, which indicates that the dispersion interaction is predominantly important over other interactions. The large red shift of the C₆₀ spectrum in the benzene solution from our gas-phase emission spectrum appears to be mainly governed by the dispersion interaction, merely enhanced by the large polarizability of the solvent, benzene. Likewise, the even larger spectral shift in the solid film should be due to the extremely large polarizability of C₆₀, which also acts as “solvent” in the solid phase.

At this point, we want to point out that several groups have already observed broad emission in the range of the visible and near-infrared light from the vapor-phase C₆₀ highly excited by multiphoton absorption^{8,9} and laser desorption.¹² They assigned the broad emission as the blackbody radiation from vibrationally hot C₆₀, whose temperature was estimated to be thousands of Kelvin, with the understanding that the blackbody radiation is one of the efficient cooling mechanisms for the super-hot C₆₀.^{27–30} From the fluence dependence of the emission intensity, Heszler et al.⁸ suggested that two or three photons at 193 nm were involved in the heating of C₆₀, and that the blackbody radiation reflected an internal temperature of 2180–3000 K. As the super-hot C₆₀ cooled, the spectrum of the blackbody radiation shifted to the red, and thus no decay time could be defined.

It is to be noted that the emission spectrum of our work is not at all related with blackbody radiation. First of all, the absorbed photon energy is not enough to give visible emission, even if we take the initial temperature of C₆₀ into consideration. The initial temperature of C₆₀ is estimated to be 4.2 eV at 800 K,³¹ and the photon energy we used ranges from 2.33 eV (532 nm) to 4.66 eV (266 nm). Therefore, the total available internal energy is from 6.5 to 8.9 eV. The corresponding temperature is only 1000 to 1200 K,³¹ which cannot produce the kind of visible emission spectrum shown in Figure 1a, with a center wavelength of 660 nm, from blackbody radiation. Second, the time-dependent spectra in Figure 2b show no spectral change as the

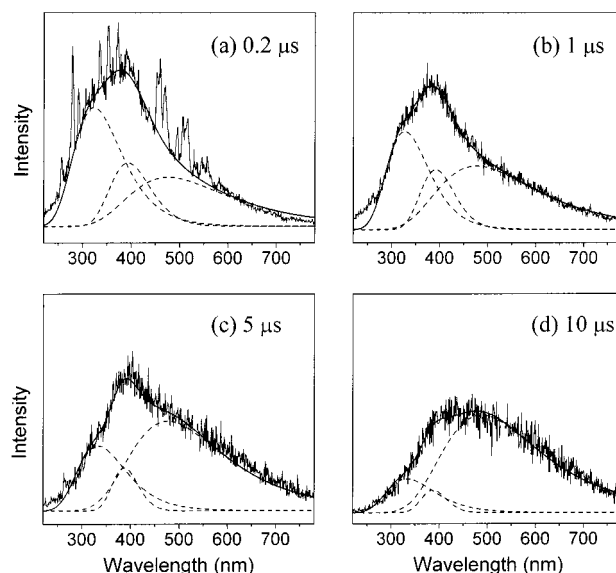


Figure 4. Time-dependent spectra of C₆₀ excited at 266 nm with high laser fluence (124 mJ/cm²). The spectra were deconvoluted into three component bands with a peak at 340 nm (α₁ band), 400 nm (α₂ band), and 500 nm (β band). At 0.2 μs, the sharp peaks are noticeably intense, but they disappear quickly so that they are almost invisible already at 1 μs. The ordinate scale is different in each figure to show the relative intensities of the component bands in detail as they decay with different decay times.

time delay is varied, indicating that there is no cooling process that shifts the spectrum as in the case of blackbody radiation.⁸ Third, we note that different excitation wavelengths led to identical spectra as we saw in Figure 2a. If the emission were blackbody radiation, different photon energies would give different internal temperatures, and yield different spectra. Finally, the decay time is too short to be that of blackbody radiation. The measured decay time of our emission is 0.95 ± 0.07 μs, which is much shorter than the known decay times of the blackbody radiation from C₆₀ (100 μs⁸) and laser-vaporized carbon clusters (tens of microseconds^{32,33}).

3. Photoluminescence from the Photofragmentation Products. The emission spectrum was found to change drastically in shape as we increased the laser fluence at 266 nm. Figure 4a shows the emission spectrum obtained with a laser fluence of 124 mJ/cm² at a delay time of 0.2 μs. It is to be noted that the peak of the emission spectrum has shifted to about 400 nm, while the band profile unmistakably suggests many component spectra. In addition, there now appear many sharp bands on top of the broad main envelope. The rest of the figures in Figure 4 show the spectra of C₆₀ at different delay times specified. We note that as the delay time becomes longer, the sharp bands disappear and the peak of the broad emission shifts to longer wavelengths. This indicates that the photoluminescence spectrum in this case is composed of different emission bands that originate from multiple chemical species generated by high-fluence laser pulse.

The Sharp Bands Due to the Swan and Fox-Herzberg Emission. To analyze the sharp features of the spectrum, we subtracted the spectrum in Figure 4b from that in Figure 4a after normalizing the peak intensities. The difference spectrum thus obtained is plotted in Figure 5. It clearly shows progressions of spectral lines with relatively narrow bandwidths. It is difficult to imagine that a very hot molecule of the size of C₆₀ with an extremely large density of states gives such sharp spectral bands as shown in Figure 5. The origin of these sharp features is thus expected to be small molecular species generated from the super-

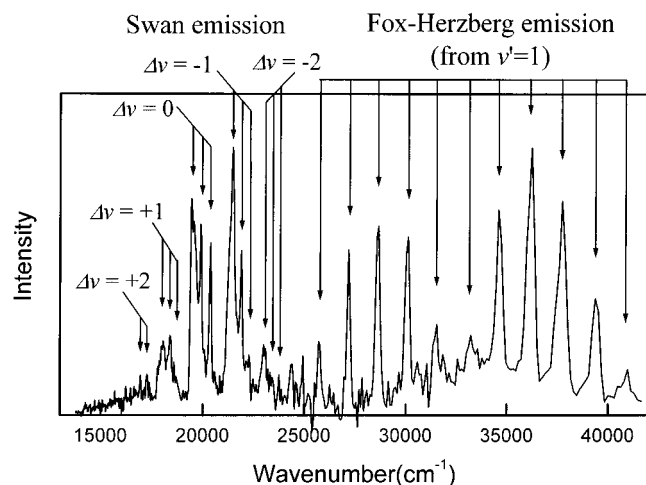


Figure 5. The difference spectrum between the spectra measured at time delays of 0.2 and 2 μ s, after normalization of the peak intensity. The spectra were obtained with the 266-nm light at a fluence of 124 mJ/cm². The sharp spectrum was assigned as the Swan (visible) and Fox-Herzberg (UV) bands of C₂. The latter bands originate only from $v' = 1$ of the excited state. (See the text.)

hot C₆₀. These sharp bands could be divided into two groups of series according to the energy difference between adjacent peaks. The lower energy series, over the spectral range of 17000–24000 cm⁻¹, turns out to be the Swan emission ($d^3\Pi_g - a^3\Pi_u$)^{34–36} of the C₂ radical, while the higher energy series, over 25000–42000 cm⁻¹, corresponds to the Fox-Herzberg bands ($e^3\Pi_g - a^3\Pi_u$)^{34,37} of the same species. The Swan bands derive from various vibronic transitions for $\Delta v = 0, \pm 1, \pm 2$, whereas the Fox-Herzberg emission is due to the transition from only one vibrational level, $v' = 1$, in the upper state ($e^3\Pi_g$) to $v'' = 1–10$ in the lower state ($a^3\Pi_u$).

The same Swan bands ($\Delta v = 0, \pm 1, \pm 2$) have also been observed from the C₂ generated from C₆₀ by laser desorption,¹² microwave plasma,¹¹ and laser excitation.⁷ In addition, the Swan emission was detected in the vaporization of graphite by irradiation of high power laser pulses.^{32,38,39} It suggests that the excited state $d^3\Pi_g$ of C₂ is readily generated from super-hot C₆₀ and graphite, regardless of the method of excitation.

On the other hand, the Fox-Herzberg emission has never been observed so far from C₂ following the fragmentation of C₆₀. More surprisingly, the emission came from only one vibrational level ($v' = 1$) of the upper state $e^3\Pi_g$. It turns out that this seemingly peculiar phenomenon is not due to a production mechanism with some propensity for $v' = 1$, but due to the coincidence in the energy of the 266-nm pump with that of the transition between $v'' = 2$ ($a^3\Pi_u$) and $v' = 1$ ($e^3\Pi_g$) levels of the C₂ molecule. Previous mass spectrometric studies^{31,40} have shown that the fragmentation of C₂ occurred with the 266-nm laser pulses at a fluence as low as 10 mJ/cm². In our case, the C₂ molecule that is evaporated from C₆₀ during the 6-ns duration of the pump pulse absorbs another 266-nm photon of the same pulse, and undergoes a transition to the $v' = 1$ state of the electronically excited $e^3\Pi_g$ state. Emission from this specific vibrational level appears as the Fox-Herzberg bands observed in our spectrum.

The time profile of the Swan and Fox-Herzberg bands could not be measured because the scattered pump light had a high intensity at short time delays. The decay time was roughly estimated to be shorter than 1 μ s from the time-dependent spectra of Figure 4. It is known that the Swan band has a short natural lifetime of about 100 ns,^{41–44} but the measured decay

time for the Swan band observed in the photofragmentation of C₆₀ was longer than its natural lifetime.^{7,9,12} This is because the fragmentation (or evaporation) of C₂ is of a delayed nature.^{7,9} The temporal profile of the Swan emission is known to be considerably affected by experimental conditions such as laser fluence and initial phase (vapor or solid) of C₆₀; for example, the reported decay times range from 140 ns and 5 μ s (193 nm, 300 mJ/cm², vapor),⁷ to 300 ns and 50 μ s (532/1064 nm, 1.5 J/cm², vapor),⁹ and to shorter than 1 μ s (308 nm, 20–200 mJ/cm², laser-desorbed film).¹² In the present work, we used a relatively low fluence of the 266-nm light with a maximum of 155 mJ/cm², which may explain the similar decay times of our work with that of ref 12 (<1 μ s). To our knowledge, the lifetime of the Fox-Herzberg transition has not been measured experimentally yet. We just propose that its lifetime could be also hundreds of nanoseconds, based on the fact that the Fox-Herzberg emission disappears completely after 1 μ s in Figure 4.

The Component Bands for the Broad Background Emission Spectrum. To resolve the broad underlying emission in all the spectra of Figure 4, it was deconvoluted by three component Gaussian bands, each centered at 340 nm (29400 cm⁻¹, α_1 band), 400 nm (25000 cm⁻¹, α_2 band), and 500 nm (20000 cm⁻¹, β band). The deconvolution of the spectrum was first performed in the linear energy scale in wavenumber, and then re-transformed into the wavelength scale. In all the deconvolution schemes we have tried, the variation in the center wavelengths remained within ± 5 nm. The α_1 and α_2 bands decay nearly together, and much faster than the low-energy β band, which retains a significant intensity even at 10 μ s.

We also measured the emission at different laser fluences, and the results are shown in Figure 6. Again, the broad background emission was deconvoluted by the same three component bands, which yielded good fitting again. We then plotted the intensity of each band as a function of the laser fluence as a log–log plot in Figure 7. They all give an excellent linear plot, with a similar slope between the α_1 and α_2 bands, and a totally different one for the β band. The similar slopes between the two α bands and their similar temporal decay suggest that these two bands could share a common origin different from that of the β band. The slope of about 3.5, or larger than 3, for the α_1 and α_2 bands suggests that these bands result from processes involving four or more photons at 266 nm, while it appears that the β band requires only two or more photons. From the temporal profile at 500 nm (not shown), the decay time of the β band was measured to be 35 ± 3 μ s. On the other hand, the α bands had a decay time of 3.4 ± 0.5 μ s. The origins of these component bands are to be discussed later.

4. Photoluminescence upon High Fluence Excitation at 355 nm. Photoluminescence spectra of C₆₀ excited by a high-fluence 355-nm light are shown in Figure 8 at different time delays. Noteworthy is the fact that the sharp Swan and Fox-Herzberg bands are not seen any longer by the 355-nm excitation, although the underlying broad band can still be fitted with the same three component bands as before. The α_1 and α_2 bands at around the same positions as before, i.e., 340 and 400 nm, decay nearly simultaneously to zero in 50 μ s, while the β band at 500 nm decays much more slowly. The fluence dependence of the emission intensity was measured at different wavelengths again, and for example, a log–log plot at 390 nm is shown in Figure 8d. Again, we have a good linear behavior, with a slope of 5.9 in this case. It means that the α_1 and α_2 bands are due to a six-photon process, which amounts to the

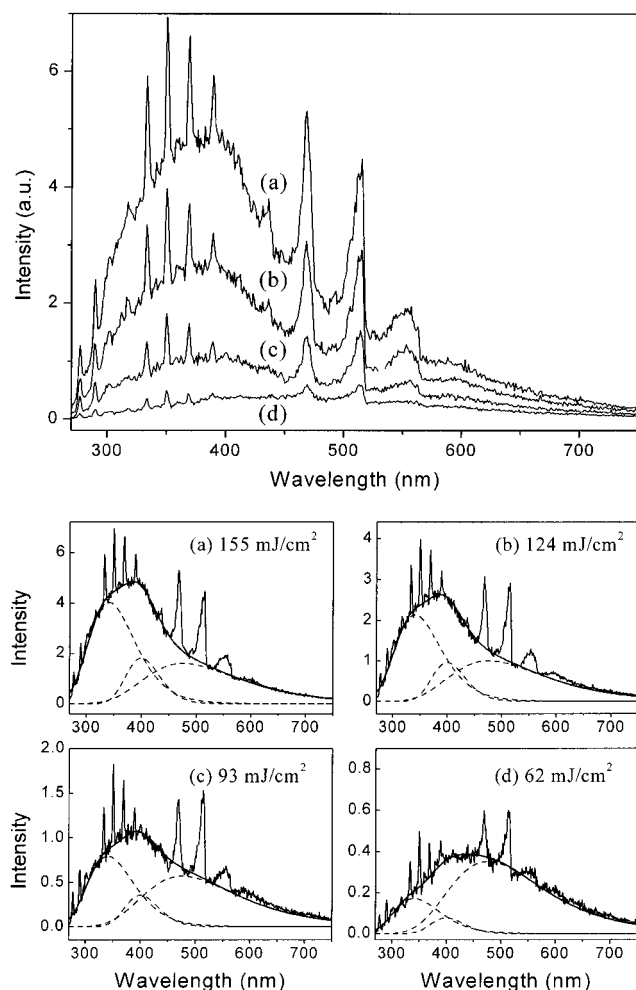


Figure 6. Fluence-dependent spectra excited by the 266-nm light at a time delay of 200 ns. In the lower panels, the broad underlying spectrum is deconvoluted into component spectra. The α_1 and α_2 bands show nearly identical fluence dependence, different from that of the β band. The ordinate scale is different in each figure from (a) to (d) to show the relative intensities of the component bands in detail.

energy of about four photons at 266 nm. On the other hand, the β band exhibited a power law exponent of about three, whose energy is equivalent to that of two photons at 266 nm. We thus realize that the total amount of energy for these bands is nearly identical regardless of the wavelength of the light used. Moreover, the measured decay time of the α_1 and α_2 bands by 355 nm was 3.4 μ s, which is the same as that measured by the 266-nm light, while the β band also showed the same decay time of 35 μ s as obtained by the 266-nm light. We therefore conclude that the excitation by the 355-nm light produces the same emitting species as the excitation by the 266-nm light for all three components bands except for the sharp Swan and Fox-Herzberg bands.

5. Generation Mechanisms of Emitting Species upon Photofragmentation. The fate of an isolated C₆₀ molecule excited by multiple photons follows two generally different paths: a prompt process such as direct ionization, direct fragmentation, and luminescence, and a delayed process such as delayed ionization, delayed fragmentation, and blackbody radiation. The prompt process occurs before the absorbed photon energy is fully thermalized, while the delayed process occurs after a thermal equilibrium is reached by energy transfer between electronic and vibrational states. Since all these processes are competing differently during and after the laser pulse, the rate

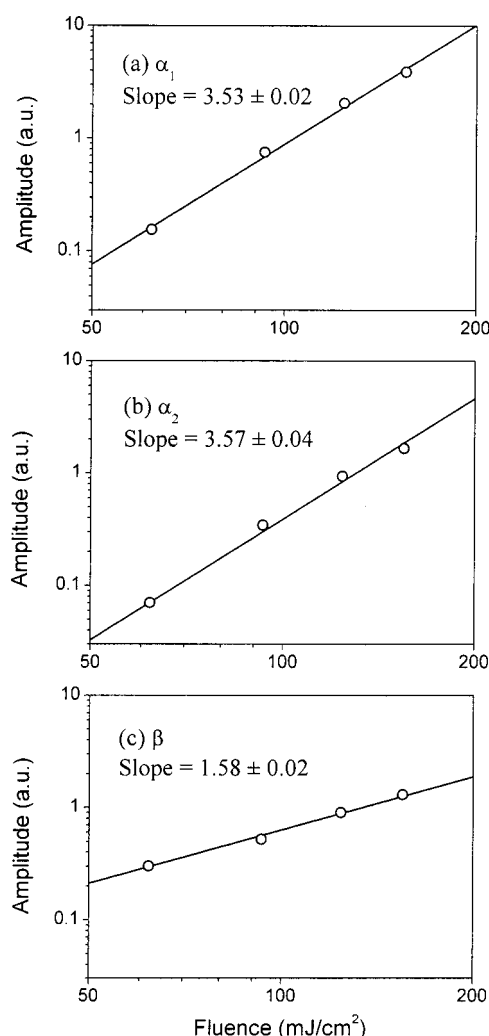


Figure 7. Log-log plot of the amplitude of the deconvoluted band of Figure 6 against the laser fluence for the (a) α_1 , (b) α_2 , and (c) β band.

of a process depends strongly on the excitation conditions such as the wavelength and fluence of the laser and the initial phase of C₆₀.

Neutral Fragmentation. It is believed that the neutral fragmentation reaction $C_{60} \rightarrow C_{58} + C_2$ is one of the major routes to generate the C₂ molecule. The minimum energy required for this process is the difference between the dissociation energy and the initial internal energy of C₆₀. Although the dissociation energy for this reaction is still uncertain¹³ between a high value of 10 to 12 eV and a lower one of about 4.5 eV, the former is more of a currently accepted value on the basis of recent studies.^{45–47} The calculated vibrational energy of C₆₀ is 0.5 eV at 300 K and 4.2 eV at 800 K, the latter being the typical temperature for C₆₀ in our effusive beam source.³¹ Therefore, if we take the dissociation energy to be 11 eV, an additional energy in excess of 6.8 eV is required to generate C₂, for which the energy of a single photon at 266 nm (4.66 eV) or 355 nm (3.50 eV) is not sufficient. Two photons are needed just to produce C₂ at both wavelengths.

For the Fox-Herzberg band emission, one additional 266-nm photon is needed to excite the C₂ molecule within the duration of the laser pulse (6 ns). Figure 9, parts a and b, show the log-log plot of the intensity of the Fox-Herzberg band as a function of laser fluence at 333 and 350 nm, respectively. The slopes come out to be 2.6 and 2.3, which indicates that at least three photons of the 266-nm light were used for the Fox-

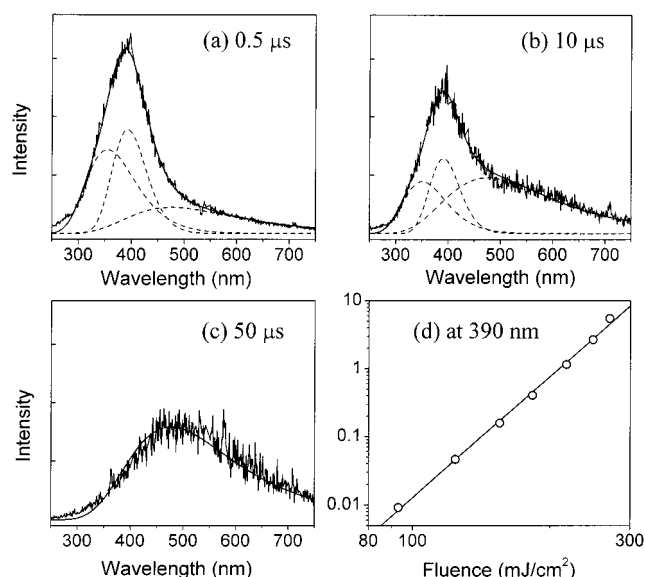


Figure 8. Time-dependent spectra of C_{60} excited by the 355-nm light with a high laser fluence of 280 mJ/cm^2 , measured at (a) $0.5 \mu\text{s}$, (b) $10 \mu\text{s}$, and (c) $50 \mu\text{s}$. The ordinate scale is different in each figure to show the relative intensities of the component bands in detail as they decay with different decay times. (d) A log-log plot of the emission intensity measured at 390 nm against the laser fluence of the 355-nm light. The fitted slope of 5.9 ± 0.1 indicates that the emission at the α_1 and α_2 bands needs six photons or more.

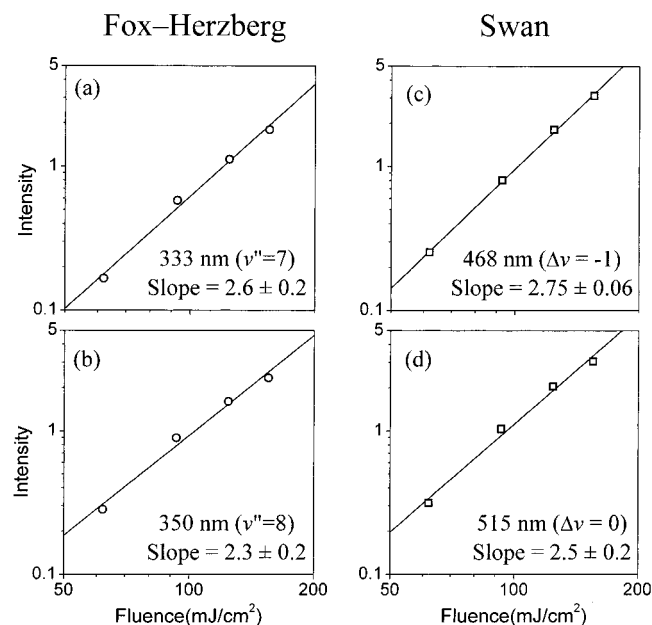


Figure 9. Log-log plots of the intensity of a few sharp emission bands against the laser fluence of the 266-nm light at the time delay of 200 ns. Intensities of emission for the sharp bands were obtained by the subtraction of intensities of the underlying broad emission after the normalization of their peak intensity.

Herzberg emission and that at least two of these were used for prompt generation of the C_2 molecule on the neutral fragmentation path. This agrees with our earlier conclusion.

Likewise, the fluence dependence of the Swan band intensities at 468 and 515 nm is shown in Figure 9, parts c and d, which gives power law exponents of 2.75 and 2.5. Since the minimum energy required for the Swan emission is 19000 cm^{-1} or 2.4 eV (Figure 5), two or three photons at 266 nm (9.32 or 13.98 eV) should be sufficient to overcome the necessary energy, $(11 + 2.4 - 4.2) \text{ eV} = 9.2 \text{ eV}$. Two-photon absorption in this

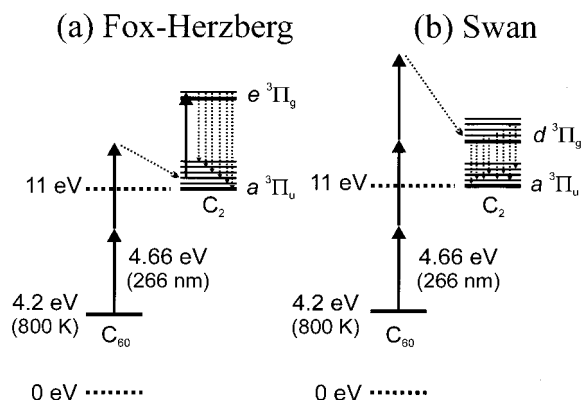


Figure 10. The energy diagram (drawn to scale) for the mechanism of the Swan and Fox-Herzberg emission by the C_2 molecule produced from super-hot C_{60} by multiphoton absorption of the 266-nm light. The dissociation energy of C_2 from C_{60} was assumed to be 11 eV, while the initial internal energy was assumed to be 4.2 eV at 800 K. (See the text.)

case would mean, however, that the C_2 molecule takes away at least 2.4 eV while the remaining C_{58} keeps only 0.12 eV or less, which is very unlikely in a purely statistical energy relaxation process. Therefore, the Swan emission is expected to require three or more photons, which is in agreement with our power law exponents of 2.75 and 2.5.

Similar Swan bands have been reported from multiphoton ionization of the C_{60} vapor at 193 nm (300 mJ/cm^2 , 17 ns),⁷ which decayed with characteristic times of 140 ns and $5 \mu\text{s}$, corresponding respectively to the prompt and delayed fragmentation. These two different modes of decay also had rather different power law exponents of 2.2 and 3.1, respectively. On the contrary, as shown in the time-dependent spectra of Figure 4, our Swan emission disappears virtually altogether well within $1 \mu\text{s}$, leaving no trace of a slow-decaying component behind. Thus, the delayed part of the Swan emission does not seem to contribute to our Swan bands, possibly because of our low laser fluence, which is not sufficient to open the delayed emission channel.

Since our Fox-Herzberg emitting state ($e^3\Pi_g$, $v' = 1$) of C_2 has the energy of 41000 cm^{-1} or 5.1 eV above the $a^3\Pi_u$ state, the minimum energy required to observe this emission band is $(11 + 5.1 - 4.2) \text{ eV} = 11.9 \text{ eV}$. Thus, three photons at 266 nm (13.98 eV) should be sufficient to dissociate the C_2 unit from C_{60} and excite it to the $e^3\Pi_g$ state to result in the Swan emission. Again, despite such energetics, a mere three-photon process is not likely because of the same reason as before; when a C_2 molecule is evaporated from C_{60} , the $e^3\Pi_g$ state of C_2 would take at least 5.1 eV, whereas the remaining C_{58} would be left with only 2.1 eV or less. A diagram showing the energetics for the emission of the Fox-Herzberg and Swan bands is given in Figure 10 as a simple summary of our mechanisms.

Ionic Fragmentation. Another mechanism for fragmentation, involving the ionic species as in $C_{60}^+ \rightarrow C_{58}^+ + C_2$, has also been proposed for the generation of C_2 .^{13,47-49} Because the ionization energy of C_{60} (7.61 eV) is higher than that of C_{58} (7.07 eV)⁵⁰ by 0.54 eV, the C_2 dissociation energy from the C_{60}^+ ion is lower than that from the neutral C_{60} by 0.54 eV, and we take it to be 10.5 eV in simple calculations. Hence, the minimum energy required for generation of C_2 in this mechanism is about $(7.6 + 10.5 - 4.2) \text{ eV} = 13.9 \text{ eV}$, including the ionization energy of 7.6 eV for C_{60} . Since this energy is only marginally smaller than that of three photons at 266 nm and we need another photon to excite the molecule for the Fox-Herzberg or Swan emission, the total number of photons needed

at 266 nm would be four or larger. These numbers are significantly larger than the power law exponent we measured, 2.3–2.75, in Figure 9. It suggests that the ionic pathway is not a very likely mechanism in our experiment to generate the C_2 molecule that gives rise to the Swan and Fox-Herzberg bands.

The absence of the sharp emission bands by the 355-nm excitation does not necessarily mean that photoexcited C_{60} does not produce C_2 at this wavelength. The fluence dependence shown in Figure 8d indicates that the emission at 390 nm needs six photons at 355 nm, with a total energy of 20.9 eV. This is a sufficient energy not only to overcome the neutral fragmentation energy barrier for C_2 (~ 11 eV) but also to reach the Swan-emitting state ($11 + 2.4 = 13.4$ eV). Deng et al.⁵¹ observed C_{58}^+ ions readily at a fluence of 29 mJ/cm² using an unfocused 355-nm light, and argued that the C_2 fragmentation could compete with delayed ionization at a high fluence (> 100 mJ/cm²). Neither Swan nor Fox-Herzberg emission was observed in the present study, however, with a fluence of up to 230 mJ/cm² for the 355-nm light. Consequently, we suggest that although the nonemitting C_2 molecule could be readily produced by the 355-nm photons, creation of electronically excited (or emitting) states of C_2 does not occur efficiently. Nevertheless, it needs to be pointed out that the 355-nm light should produce the emitting-type C_2 molecules at a much higher fluence, because the Swan emission has been observed at 532 nm with a fluence of 1.5 J/cm².⁹

Origins of the Broad Background Emission. We now discuss the origins of the component bands that comprise the broad background emission of Figures 4, 6, and 8. The α_1 and α_2 bands exhibited nearly identical temporal decay as shown in Figure 4 for the 266-nm case and Figure 8 for the 355-nm case. Their fluence dependence was also nearly the same (Figures 6 and 7). It is likely that they have a common origin, or at least a common pathway to reach their emitting state.

As mentioned earlier, radiative cooling by blackbody radiation has been proposed as one of the likely cooling processes for a super-hot C_{60} molecule.^{8–10,12,27–31} Heszler et al.⁸ observed blackbody radiation from C_{60} that absorbed three photons (with a power law exponent of 2.8) at 193 nm, and estimated its internal temperature to be in the range of 2050 to 2450 K. In our experiment, the total photon energy of the four photons at 266 nm for the α_1 and α_2 bands was comparable at 18.64 eV. With the initial internal energy of 4.2 eV, a total internal energy of 22.8 eV gives a vibrational temperature of 2400 K from the equation in ref 32, if the entire energy were to be fully converted into equilibrium vibrational energy in the electronic ground state. This temperature is quite close to that of Heszler et al.'s super-hot C_{60} in their experiment. Our α_1 and α_2 bands have peaks at much shorter wavelengths, however, than their blackbody radiation peak, i.e. 340 and 400 nm vs 500 nm or longer. It suggests that the α_1 and α_2 bands are not due to blackbody radiation. Another possibility is photoluminescence from a higher electronically excited state of C_{60} , but it is unlikely that its higher electronic state lives as long as 3.4 μ s because a large molecule like C_{60} should have an extremely fast relaxation rate to the S_1 state.

It is also possible that the two bands are due to emission from the neutral fragments (C_{58} , C_{56} , and so on), the C_{60}^+ ion, or the ionic fragments (C_{58}^+ , C_{56}^+ , and so on). Energetically, because the onset energy of the α_1 and α_2 bands is 5.0 eV (250 nm), the remaining energy of 17.8 eV is available for fragmentation, ionization, or both. All three species of C_{58} , C_{60}^+ , and C_{58}^+ can be emitters of the α_1 and α_2 bands since the energy of C_2 fragmentation from neutral C_{60} is ~ 11 eV, the ionization

energy of C_{60} is 7.6 eV, and the energy of C_2 fragmentation from ionic C_{60}^+ is ~ 18 eV. On the contrary, other smaller fragments cannot contribute to the emission because the energy required for their generation through a further dissociation is much higher than is available. At this stage, we cannot determine which of the above species is the origin of the bands; rather, we can only propose that the α_1 and α_2 bands come from the excited states of one or more of those species.

It is quite obvious that the β band is distinctly different from the α_1 and α_2 bands in terms of the decay time and laser fluence dependence, and thus should have a different origin. The β band showed a decay time of 35 μ s upon excitation by both the 266-nm and 355-nm lights, while the number of photons needed was two at 266 nm and three at 355 nm. It means that the minimum energy required for the β band is 13.5 eV, which yields a vibrational temperature of about 1600 K. This temperature is not quite high enough to give the blackbody radiation with a peak at 500 nm of our spectrum. The decay time of 35 μ s is also quite shorter than Heszler et al.'s ~ 100 μ s.⁸ Nevertheless, it is still possible that the β band is due to blackbody radiation, considering the breadth of the spectrum and also the difference in the detection system and excitation scheme between ours and those of Heszler et al. On the other hand, following the same argument as before, we estimate the minimum energy required for the generation of the emitter of this band is 9.4 eV because the onset of the β band is 300 nm or 4.1 eV. Both C_{60}^+ and C_{58} could be the carrier of the emission, but not C_{58}^+ as in the case of the two α bands. At this point, we cannot determine whether the origin of the β band is blackbody radiation or photoluminescence from the excited states of C_{60}^+ and C_{58} or both.

IV. Conclusion

The genuine photoluminescence spectrum of the gas-phase C_{60} was obtained for the first time. It was explicitly shown that the origin of the photoluminescence was the S_1 state of the isolated neutral C_{60} by the following arguments: (1) the measured sublimation enthalpy was nearly identical to the known value for C_{60} ; (2) the photoluminescence was confirmed to be due to a single photon process from its linear fluence dependence; (3) the photoluminescence spectrum did not depend on the excitation wavelength; (4) the spectral shape did not change as the delay time was varied; and (5) the temporal decay was almost perfectly single-exponential. Additionally, it was shown that the emission was neither blackbody radiation nor phosphorescence. The measured photoluminescence decay time of 0.95 μ s was about 1000 times longer than in solution.

With high-fluence laser pulses at 266 nm, drastically different emission spectra resulted from multiphoton absorption. The fast-decaying, sharp emission bands were assigned as the Fox-Herzberg (from $v' = 1$) and Swan ($\Delta v = 0, \pm 1$, and ± 2) bands of C_2 dissociated from super-hot C_{60} . The long-lived broad band was deconvoluted into three component bands. Two of them, with a peak at around 340 and 400 nm (denoted as α_1 and α_2 , respectively), originated from four-photon excitation and had a decay time of 3.4 ± 0.5 μ s. The other band at around 500 nm (denoted as β) required two photons and had a decay time of 35 ± 3 μ s. Excitation at 355 nm with a high-fluence light led to a similar broad emission band with the same three component bands, but no emission from C_2 was observed. From the analysis of the power dependence and decay times, the component emission bands were attributed to C_{58} , C_{60}^+ , and C_{58}^+ in the case of the two α bands and to C_{58} and C_{60}^+ as well as blackbody radiation in the case of the β band.

Acknowledgment. This work was supported by the National Creative Research Initiatives Program (99-C-CT-01-C-50) of the Ministry of Science and Technology.

References and Notes

- (1) Brady, B. B.; Beiting, E. J. *J. Chem. Phys.* **1992**, 97, 3855.
- (2) Gong, Q.; Sun, Y.; Huang, Z.; Zhou, X.; Gu, Z.; Qiang, D. *J. Phys. B: At. Mol. Opt. Phys.* **1996**, 29, 4981.
- (3) Smith, A. L. *J. Phys. B: At. Mol. Opt. Phys.* **1996**, 29, 4975.
- (4) Dai, S.; Toth, L. M.; Cul, G. D. D.; Metcalf, D. H. *J. Chem. Phys.* **1994**, 101, 4470.
- (5) Coheur, P. F.; Carleer, M.; Colin, R. *J. Phys. B: At. Mol. Opt. Phys.* **1996**, 29, 4987.
- (6) Leach, S.; Vervloet, L.; Desprès, A.; Bréheret, E.; Hare, J. P.; Dennis, T. J.; Kroto, H. W.; Taylor, R.; Walton, D. R. N. *Chem. Phys.* **1992**, 160, 451.
- (7) Heszler, P.; Carlsson, J. O.; Demirev, P. *Phys. Rev. B* **1996**, 53, 12541.
- (8) Heszler, P.; Carlsson, J. O.; Demirev, P. *J. Chem. Phys.* **1997**, 107, 10440.
- (9) Arepalli, S.; Scott, C. D.; Nikolaev, P.; Smalley, R. E. *Chem. Phys. Lett.* **2000**, 320, 26.
- (10) Vostrikov, A. A.; Dubov, D. Y.; Agarkov, A. A. *JETP Lett.* **1996**, 63, 963.
- (11) Gruen, D. M.; Liu, S.; Krauss, A. R.; Pan, X. *J. Appl. Phys.* **1994**, 75, 1758.
- (12) Mitzner, R.; Campbell, E. E. B. *J. Chem. Phys.* **1995**, 103, 2445.
- (13) Lifshitz, C. *Int. J. Mass Spectrom.* **2000**, 198, 1.
- (14) Campbell, E. E. B.; Levine, R. D. *Annu. Rev. Phys. Chem.* **2000**, 51, 65.
- (15) Turro, N. J. *Modern Molecular Photochemistry*; Benjamin/Cummings: Menlo Park, 1978; p 103.
- (16) Haufler, R. E.; Wang, L.-S.; Chibante, L. P. F.; Jin, C.; Conceicao, J.; Chai, Y.; Smalley, R. E. *Chem. Phys. Lett.* **1991**, 179, 449.
- (17) Hung, W.-C.; Ho, C.-D.; Liu, C.-P.; Lee, Y.-P. *J. Phys. Chem.* **1996**, 100, 3927.
- (18) van den Heuvel, D. J.; Chan, I. Y.; Groenen, E. J. J.; Schimidt, J.; Meijer, G. *Chem. Phys. Lett.* **1994**, 231, 111.
- (19) Catalán, J. *Chem. Phys. Lett.* **1994**, 223, 159.
- (20) Haufler, R. E.; Chai, Y.; Chibante, L. P. F.; Fraelich, M. R.; Weisman, R. B.; Curl, R. F.; Smalley, R. E. *J. Chem. Phys.* **1991**, 95, 2197.
- (21) Sassara, A.; Zerza, G.; Chergui, M.; Negri, F.; Orlandi, G. *J. Chem. Phys.* **1997**, 107, 8731; and references therein.
- (22) Sassara, A.; Zerza, G.; Chergui, M. *J. Phys. B: At. Mol. Opt. Phys.* **1996**, 29, 4997.
- (23) Kim, D.; Lee, M.; Suh, Y. D.; Kim, S. K. *J. Am. Chem. Soc.* **1992**, 114, 4429.
- (24) Lee, M.; Song, O.-K.; Seo, J.-C.; Kim, D.; Suh, Y. D.; Jin, S. M.; Kim, S. K. *Chem. Phys. Lett.* **1992**, 196, 325.
- (25) Lakowicz, J. R. *Principles of Fluorescence Spectroscopy*; Plenum: New York and London, 1983; p 187.
- (26) Reichardt, C. *Solvents and Solvent Effects in Organic Chemistry*, 2nd. ed.; VCH: Weinheim, 1988; p 301.
- (27) Kolodney, E.; Tsipinyuk, B.; Budrevich, A. *J. Chem. Phys.* **1995**, 102, 9263.
- (28) Kolodney, E.; Budrevich, A.; Tsipinyuk, B. *Phys. Rev. Lett.* **1995**, 74, 510.
- (29) Hansen, K.; Campbell, E. E. B. *J. Chem. Phys.* **1996**, 104, 5012.
- (30) Chupka, W. A.; Klotz, C. E. *Int. J. Mass Spectrom. Ion Processes* **1997**, 167/168, 595.
- (31) Wurz, P.; Lykke, K. R. *J. Phys. Chem.* **1992**, 96, 10129.
- (32) Rohlfing, E. A. *J. Chem. Phys.* **1988**, 89, 6103.
- (33) Balm, S. P.; Hallett, R. A.; Allaf, A. W.; Stace, A. J.; Kroto, H. W. *Int. J. Mod. Phys. B* **1992**, 6, 3757.
- (34) Herzberg, G. *Molecular Spectra and Molecular Structure, Vol. 1. Spectra of Diatomic Molecules*; Van Nostrand Reinhold: New York, 1950.
- (35) Winicur, D. H.; Hardwick, J. L.; Murphy, S. N. *Combust. Flame* **1983**, 53, 93.
- (36) Danylewych, L. L.; Nicholis, R. W. *Proc. R. Soc. London A* **1974**, 339, 197.
- (37) Fox, J. G.; Herzberg, G. *Phys. Rev.* **1937**, 52, 638.
- (38) Abhilasha.; Thareja, R. K. *Phys. Lett. A* **1993**, 184, 99.
- (39) Arepalli, S.; Scott, C. D. *Chem. Phys. Lett.* **1999**, 302, 139.
- (40) Wurz, P.; Lykke, K. R. *Chem. Phys.* **1994**, 184, 335.
- (41) Stark, G.; Davis, S. D. *Z. Phys. A* **1985**, 321, 75.
- (42) Bauer, W.; Becker, K. H.; Bielefeld, M.; Meuser, R. *Chem. Phys. Lett.* **1986**, 123, 33.
- (43) Naulin, C.; Costes, M.; Dorthé, G. *Chem. Phys. Lett.* **1988**, 143, 496.
- (44) Urdahl, R. S.; Bao, Y.; Jackson, W. M. *Chem. Phys. Lett.* **1988**, 152, 485.
- (45) Hansen, K.; Echt, O. *Phys. Rev. Lett.* **1997**, 78, 2337.
- (46) Boese, A. D.; Scuseria, G. E. *Chem. Phys. Lett.* **1998**, 294, 233.
- (47) Matt, S.; Echt, O.; Sonderegger, M.; David, R.; Scheier, P.; Laskin, J.; Lifshitz, C.; Märk, T. D. *Chem. Phys. Lett.* **1999**, 303, 379.
- (48) O'Brien, S. C.; Heath, J. R.; Curl, R. F.; Smalley, R. E. *J. Chem. Phys.* **1988**, 88, 220.
- (49) Hohmann, H.; Callegari, C.; Furrer, S.; Grosenick, D.; Campbell, E. E. B.; Hertel, I. V. *Phys. Rev. Lett.* **1994**, 73, 1919.
- (50) Zimmerman, J. A.; Eyler, J. R.; Bach, S. B. H.; McElvany, S. W. *J. Chem. Phys.* **1991**, 94, 3556.
- (51) Deng, R.; Echt, O. *J. Phys. Chem. A* **1998**, 102, 2533.
- (52) Tokmakoff, A.; Haynes, D. R.; George, S. M. *Chem. Phys. Lett.* **1991**, 186, 450.
- (53) Pan, C.; Sampson, M. P.; Chai, Y.; Hauge, R. H.; Margrave, J. L. *J. Phys. Chem.* **1991**, 95, 2944.
- (54) Abrefah, J.; Olander, D. R.; Balooch, M.; Siekhaus, W. J. *Appl. Phys. Lett.* **1992**, 60, 1313.
- (55) Mathews, C. K.; Baba, M. S.; Narasimhan, T. S. L.; Balasubramanian, R.; Sivaraman, N.; Srinivasan, T. G.; Rao, P. R. V. *J. Phys. Chem.* **1992**, 96, 3566.
- (56) Popović, A.; Dražić, G.; Marcel, J. *Rapid Commun. Mass Spectrom.* **1994**, 8, 985.
- (57) Piacente, V.; Gigli, G.; Scardala, P.; Giustini, A.; Ferro, D. *J. Phys. Chem.* **1995**, 99, 14052.